Efficient local atomic packing in metallic glasses and its correlation with glass-forming ability

D. Ma,[1,*] A. D. Stoica,[1] X-L. Wang,[1] Z. P. Lu,[2] M. Xu,[3] and M. Kramer[3]
[1]*Neutron Scattering Science Division, Oak Ridge National Laboratory, Oak Ridge, Tennessee 37831, USA*
[2]*State Key Laboratory for Advanced Metals and Materials, University of Science and Technology Beijing, Beijing 100083, China*
[3]*Materials and Engineering Physics, Ames Laboratory, Ames, Iowa 50011, USA*
(Received 29 January 2009; published 15 July 2009)

We have probed local atomic structure of Zr-Cu metallic glasses using time-of-flight neutron and synchrotron x-ray diffraction techniques with high resolution. Our results provide evidence for a scheme of efficient local atomic packing where atomic clusters encompass multiple types of atoms in the first coordination shell. We also demonstrate experimental evidence of a strong correlation between the number of unlike atom bonds and the glass-forming ability. Our findings may provide insights into a broad range of scientific problems where efficient space filling by packing spheres is essential.

DOI: 10.1103/PhysRevB.80.014202 PACS number(s): 61.05.J−, 75.50.Kj, 75.30.Gw, 68.37.Lp

I. INTRODUCTION

A liquid freezes into a glass when bypassing crystallization upon cooling. The slower an atom moves around in the liquid, the more likely the atom escapes the capture of crystallization. In glass-forming liquids such as polymer and silica liquids, rather than individual random walk, atoms are encaged in molecular units (such as the SiO_4 tetrahedra in liquid silica[1]) which, in a collective motion manner, reduce dramatically the atomic mobility.[2] These local structural units thus account for the excellent glass-forming ability of the liquids and remain as the building blocks of polymer and silica glasses.[2,3] Analogously, metallic glasses also exhibit signs of local structure units such as short-range orders (or solute-centered atomic clusters), as proposed in recent works of structural modeling and computer simulation.[4–6] However, there is a lack of key experimental determination of local atomic structure in metallic glasses and the correlation between local atomic packing with glass-forming ability has yet to be demonstrated experimentally over the years.

In this work, we select binary Zr-Cu glasses for a systematic investigation of local atomic packing units because of the simplicity in composition variation. This is also motivated by the recent discovery of bulk metallic glasses in this binary system, which has sparked renewed interest in understanding the structure of metallic glasses.[7–13] In fact, for this particular system, many neutron and x-ray experiments, and computer simulations have been carried out over the decades.[14–21] However, due to the difficulty in resolving partial pair-correlation functions in experiments and the uncertainty in determining the pair-wise potentials in simulations, data in the literature appear to be inconsistent and sometimes contradictory with each other. For example, Lamparter *et al.*[14] conducted neutron-scattering experiments and reported a positive Warren-Cowley (WC) short-range order coefficient (α) (Ref. 22) with respect to Cu for the $Cu_{57}Zr_{43}$ glass but Kudo *et al.*[15] determined a negative α using the same technique. This is also the case for the $Zr_{50}Cu_{50}$ glass, for which Fujiwara *et al.*[16]estimated a positive α in terms of Zr using computer simulations whereas Chen and Waseda[17] obtained a negative value of α by means of an anomalous x-ray scattering technique. We set out to attain precise determination of local atomic structure of Zr-Cu glasses hence gain clear insights into the role of local atomic packing in the glass formability. Our approach is to make complementary use of time-of-flight neutron and high-energy x-ray diffraction techniques, which provides high-resolution measurements and significant contrast variations. Furthermore, we employed a Cu-isotope substitution method in the neutron diffraction experiments to facilitate precise extraction of partial pair-correlation functions for a particular $Zr_{35.5}Cu_{64.5}$ glass and used them as references for the structure determination of other Zr-Cu glasses.

II. EXPERIMENTS

The Zr-Cu glasses of our study are $Zr_xCu_{(100-x)}$ (x=30.0, 35.5, 38.6, 41.2, 44.0, 50.0, 54.5, 60.0, 66.7, and 70.0) in the form of thin ribbons of ~50 μm thick and ~5 mm wide. The amorphous ribbons were made from rapid quenching of the melts of prealloyed Zr and Cu ingots using a melt-spinning technique. Their compositions were examined using electron probe microanalysis, which indicated a small composition variation of less than 1% from an average of 15 measurements for each tested ribbon. Thermal properties of these ribbons, including the onset of crystallization temperature (T_x), the glass transition temperature (T_g), and the liquidus temperature (T_l) were determined using differential scanning calorimetry (DSC) at a scanning rate of 20 K/min, as summarized in Table I. However, only six of the Zr-Cu glasses were used in diffraction studies, i.e., $Zr_xCu_{(100-x)}$ (x =35.5, 38.6, 44, 50, 54.5, and 60). Besides six natural Cu-containing glasses, three Cu-isotope substituted $Zr_{35.5}Cu_{64.5}$ glasses were also prepared, which are designated as $Zr_{35.5}{}^{65}Cu_{64.5}$, $Zr_{35.5}{}^{63}Cu_{64.5}$, and $Zr_{35.5}{}^{Zr}Cu_{64.5}$, respectively. The first two were made by completely substituting natural Cu with ^{65}Cu and ^{63}Cu, respectively, and the third one by partially substituting natural Cu with an appropriate amount of ^{63}Cu to match the scattering length (b) of the Cu element with that of Zr(b_{Zr}=7.16 fm). The neutron diffraction experiments were carried out on the general purpose powder diffractometer (GPPD) at Argonne National Laboratory. The scattering data, as a function of the momentum transfer q [$=4\pi \sin\theta/\lambda$ where λ is the wavelength and 2θ is the scat-

TABLE I. Summary of partial coordination numbers, Warren-Cowley coefficients[22] $\{\alpha_i=1-Z_{ij}/[c_j(Z_{ij}+Z_{ii})]\}$, thermal properties and the glass-forming ability indicators $\gamma[=T_x/(T_g+T_l)]$ and $T_{rg}(=T_g/T_l)$ of amorphous Zr-Cu alloys.

Amorphous Alloys	Z_{CuCu}	Z_{CuZr}	Z_{ZrCu}	Z_{ZrZr}	α_{Cu}	α_{Zr}	T_g (K)	T_x (K)	T_L (K)	γ	T_{rg}
$Zr_{30.0}Cu_{70.0}$							683	764	1364	0.373	0.501
$Zr_{35.5}Cu_{64.5}$	7.19	4.94	8.98	4.08	−0.048	0.03	727	773	1324	0.377	0.549
$Zr_{38.6}Cu_{61.4}$	6.12	5.40	8.59	4.75	−0.091	0.06	715	753	1299	0.374	0.550
$Zr_{41.2}Cu_{58.8}$							675	735	1222	0.387	0.552
$Zr_{44.0}Cu_{56.0}$	4.54	6.45	8.22	6.05	−0.148	0.12	674	728	1191	0.390	0.566
$Zr_{50.0}Cu_{50.0}$	3.02	7.25	7.25	7.19	−0.169	0.17	658	705	1221	0.375	0.539
$Zr_{54.5}Cu_{45.5}$	2.65	7.41	6.19	7.82	−0.147	0.18	644	694	1225	0.371	0.526
$Zr_{60.0}Cu_{40.0}$	2.03	8.03	5.36	8.01	−0.110	0.16	641	683	1222	0.367	0.525
$Zr_{66.7}Cu_{33.3}$							610	655	1290	0.345	0.473
$Zr_{70.0}Cu_{30.0}$							590	629	1289	0.335	0.458

tering angle], were collected at room temperature for 8 h for the natural Cu samples and for 24 h for the Cu-isotope-substituted samples, respectively. The total scattering patterns of the six Zr-Cu glasses were also obtained using high-energy x-ray diffraction at Advanced Photon Source (APS) of Argonne National Laboratory. The neutron and x-ray structure factors, i.e., $S_N(q)$ and $S_X(q)$, were determined using PDFgetN (Ref. 23) and PDFgetX2,[24] respectively. The reduced pair-distribution function (PDF) [$G(r)$, where r is the distance] was obtained by Fourier transforming $S(q)$,[25] $G(r)=\frac{2}{\pi}\int_0^\infty q[S(q)-1]\sin(qr)dq=4\pi r[\rho(r)-\rho_0]$, where ρ_0 is the average number density and $\rho(r)$ is the microscopic number density. Figures 1(a) and 1(b) show the $G_N(r)$ and $G_X(r)$ for the six natural Cu-containing Zr-Cu glasses, respectively. Figure 1(c) shows the $G(r)$ of the $Zr_{35.5}Cu_{64.5}$ glass obtained from neutron diffraction of Cu-isotope-substituted samples (with ^{65}Cu, ^{Nat}Cu, ^{Zr}Cu, and ^{63}Cu, respectively) and that by x-ray diffraction.

III. PDF METHODOLOGY AND DATA ANALYSIS

To extract the nearest-neighbor structure information from the first PDF peak, we have converted $G(r)$ into $T(r)$[$=4\pi r\rho(r)=4\pi\rho_0 r+G(r)$].[26] $T(r)$ can be expressed as a sum of weighted partial PDFs, i.e., $T(r)=\Sigma_i\Sigma_{j\le i}T_{ij}(r)\cdot w_{ij}$, where $T_{ij}(r)=4\pi r\rho_{ij}(r)$, and i, and j denote the ith and jth atomic species, and w_{ij} is the weight of the i-j pair. $w_{ij}=2c_ic_jb_ib_j/\langle b\rangle^2$ $(i\neq j)$ or $w_{ij}=c_ic_jb_ib_j/\langle b\rangle^2$ $(i=j)$, where c_i is the atomic fraction and b_i is the scattering length of the ith element (in the case of x ray, b_i is replaced by $f_i(0)$, the atomic scattering factor), $\langle b\rangle=\Sigma_i c_i b_i$ is the average scattering length, and $\rho_{ij}(r)$ is the partial pair-density function. In the present analysis, we consider each $T_{ij}(r)$ as a convolution between a Gaussian distribution $[T_{ga}(r)]$ and an exponential function $[T_{ex}(r)]$

$$T_{ga}(r)=\frac{1}{\sqrt{2\pi}\sigma}\exp\left[-\frac{r^2}{2\sigma^2}\right], \tag{1a}$$

$$T_{ex}(r)=\begin{cases}0, r<0\\ \beta\exp[-\beta r], r\ge 0\end{cases}, \tag{1b}$$

where σ and β are the standard deviation and the exponential decay constant, respectively. The convolution yields

$$T_{ij}(r)=\frac{a_{ij}\cdot p_{ij}}{\sigma_{ij}}\exp\left[-p_{ij}\left(\frac{r-r_{ij}}{\sigma_{ij}}-\frac{p_{ij}}{2}\right)\right]\times\Phi\left(\frac{r-r_{ij}}{\sigma_{ij}}-p_{ij}\right), \tag{2}$$

where $p_{ij}=\beta_{ij}\sigma_{ij}$, a_{ij} is the peak amplitude, r_{ij} is the peak position, and Φ is the normal cumulative distribution function, $\Phi(y)=\int_{-\infty}^{y}\frac{1}{\sqrt{2\pi}}\exp(-\frac{x^2}{2})dx$. The partial coordination number (Z_{ij}), which represents the number of the nearest-neighbor j-type atoms surrounding an i-type atom, can be obtained as

$$Z_{ij}=c_j\int_0^\infty T_{ij}(r)\cdot r dr\approx c_j a_{ij}\left(r_{ij}+\frac{1}{\beta_{ij}}\right). \tag{3}$$

For a binary Zr-Cu glass, there are three $T_{ij}(r)$s corresponding to the Cu-Cu, Cu-Zr (or Zr-Cu), and Zr-Zr correlations, respectively. Each partial has a single x-ray weight (w_{ij}^X) but may have various neutron weights (w_{ij}^N) due to the presence of isotopes. For the $Zr_{35.5}Cu_{64.5}$ glass, in addition to w_{ij}^X, four different values of w_{ij}^N have been obtained using Cu-isotope substitutions [^{65}Cu and ^{63}Cu, see Fig. 1(c)]. The resultant variation of w_{ij}^N accounts for the first PDF peak shift toward smaller r for the glass containing more ^{65}Cu because the scattering length of ^{65}Cu is more than 1.5 times that of ^{63}Cu. Using three convoluted Gaussian functions [Eq. (2)] to represent the three $T_{ij}(r)$ s, and assigning each $T_{ij}(r)$ with the corresponding neutron and x-ray weights, we have carried out a simultaneous fit to the first-shell peaks $(2.3\le r\le 3.6$ Å) of the four $T_N(r)$s and one $T_X(r)$ for the $Zr_{35.5}Cu_{64.5}$ glass (see Fig. 2). In the fitting process, we used the sum of atomic radii (1.27 and 1.58 Å for Cu and Zr atoms, respectively[27]) as the initial inputs of the peak positions (r_{ij}) and kept the specific weighting factors fixed and the same partial coordination numbers as parameters. Figure 2 shows the best fit to the $T_N(r)$s and $T_X(r)$, as well as the weighted

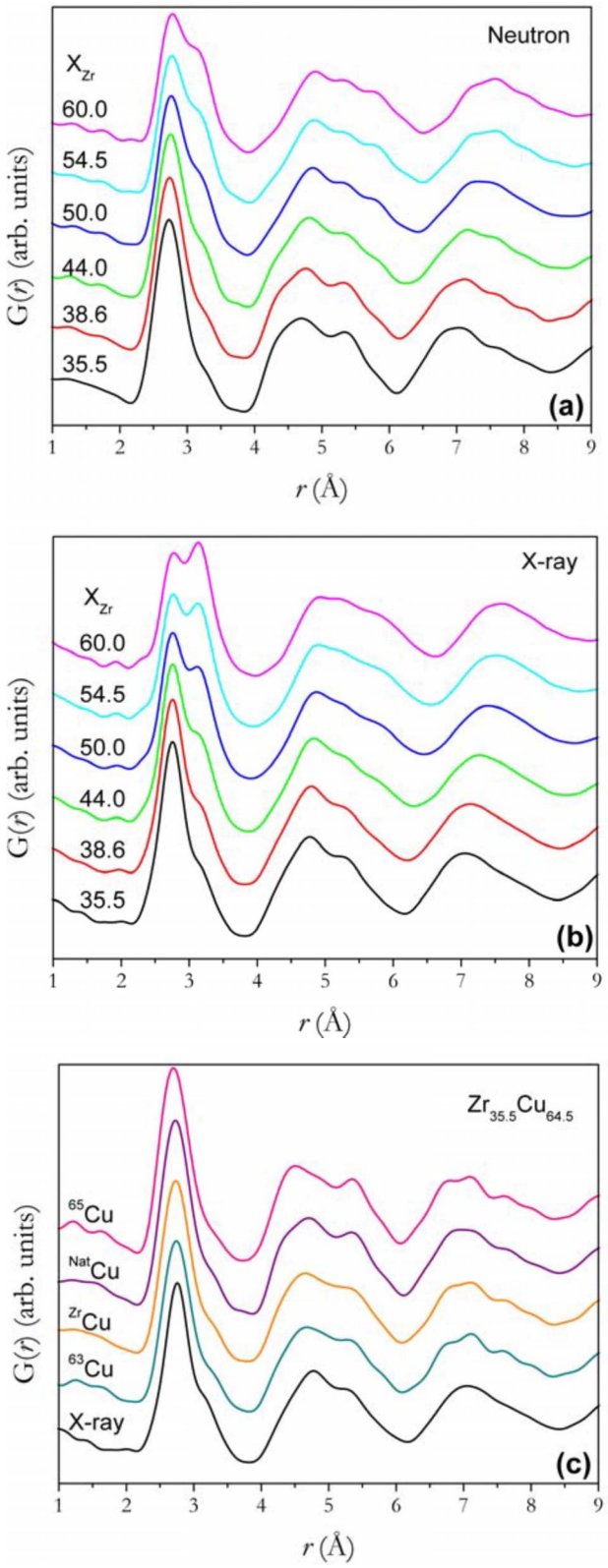

FIG. 1. (Color online) The reduced PDF $[G(r)]$ of a series of natural Cu-containing Zr-Cu glasses determined by (a) neutron and (b) x-ray diffractions. Also shown in (c) are the $G(r)$s of the $Zr_{35.5}Cu_{64.5}$ glass obtained by neutron diffraction of Cu-isotope-substituted samples (with ^{65}Cu, ^{Nat}Cu, ^{Zr}Cu, and ^{63}Cu, respectively), and x-ray diffraction of the natural Cu-containing sample.

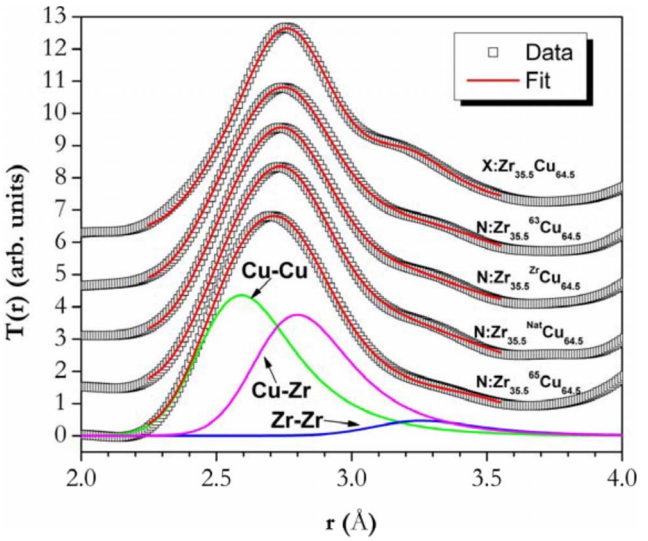

FIG. 2. (Color online) The best fit of a linear combination of convoluted Gaussian functions to the $T_N(r)$s of the $Zr_{35.5}Cu_{64.5}$ glass with Cu-isotope substitutions and to the $T_X(r)$ of the same alloy. Also shown are the extracted Zr-Zr, Zr-Cu, and Cu-Cu partials for $Zr_{35.5}{}^{65}Cu_{64.5}$.

$T_{ij}(r)$s corresponding to Cu-Cu, Zr-Cu, and Zr-Zr for the $Zr_{35.5}{}^{65}Cu_{64.5}$ glass. The fitted r_{ij} values of 2.48 and 3.13 Å for the Cu-Cu and Zr-Zr pairs, respectively, are close to the hard-sphere model prediction. As the partials do not show distinctive shapes, the best-fit data were obtained by using a constant β_{ij}(=4.81) and close values of σ_{ij} in the range of 0.12–0.15 Å. Taking into account the exponential tail of the profile, the average values for the Cu-Cu and Zr-Zr bonds amount to 2.59 and 3.26 Å, respectively, which correspond to a 2% increase relative to the hard-sphere expectation and can explain the departure of the real distribution of atoms from the ideal structure of densely packed spheres. On the other hand, the average value of the Zr-Cu bond (2.80 Å) reveals a net contraction of 2% relative to the hard-spheres limit. Therefore, the unlike atom bonds are expected to be the most stable ones in the mixture. Moreover, using the best-fit parameters obtained for the $Zr_{35.5}Cu_{64.5}$ glass as initial inputs and adjusting the weights due to the composition change, we have performed similar fits to the $T_N(r)$ and $T_X(r)$ for the other five Zr-Cu glasses. As the Cu-Cu partial does not show a well separated peak in the first PDF shell, the Cu-Cu bond length was fixed in the composition-dependent analysis. The other two bond lengths show slight shortening toward the Zr rich side, i.e., 1% and 2% for Zr-Cu and Zr-Zr, respectively.

IV. RESULTS AND DISCUSSION

The partial coordination numbers have been extracted using Eq. (3), as summarized in Table I and shown in Fig. 3. For comparison, Fig. 3 also shows the data available in the literature with respect to Cu-Cu, Cu-Zr, Zr-Cu, and Zr-Zr, respectively.[21] While the literature data exhibit rather large discrepancies with each other as we have pointed out earlier, the present work provides a systematic and consistent corre-

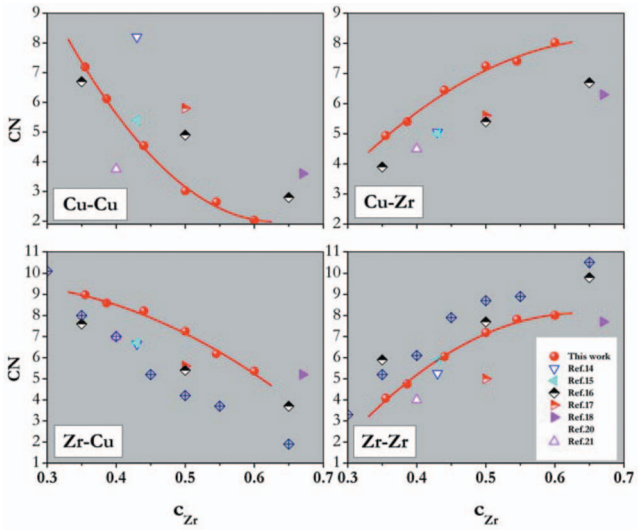

FIG. 3. (Color) Comparison of the extracted partial-coordination numbers in this work with the literature data with respect to (a) Cu-Cu, (b) Cu-Zr, (c) Zr-Cu, and (d) Zr-Zr, respectively.

lation between the coordination numbers and the glass composition.

The extracted CNs allow us to estimate the Warren-Cowley short-range order coefficient,[22] i.e., $\alpha_i = 1 - Z_{ij}/[c_j(Z_{ij}+Z_{ii})]$ where i refers to either Cu or Zr. As summarized in Table I, the WC coefficients with respect to Cu-α_{Cu} are all negative ranging from −0.05 to −0.15, whereas α_{Zr} varies between 0.03 and 0.18. This indicates that the amount of Zr atoms surrounding a Cu atom is, on average, larger than what it would be in random packing. The aggregation of Zr atoms around Cu may lead to the formation of Cu-centered clusters as revealed in previous studies.[4,6,26] To elucidate this point, we have performed an in-depth analysis of coordination numbers by extending the framework of efficient local atomic packing established by Miracle *et al.*[5] Following this concept, in a binary alloy where a type-A atom is surrounded only by type-B atoms, the maximum coordination number Z_{AB}^{T} can be determined solely upon the ratio between the radii of the atoms, $R_{AB}(=R_B/R_A)$.[5] In the case of Zr-Cu, for instance, one has $Z_{CuZr}^{T}=10.1$, $Z_{ZrCu}^{T}=16.9$, and $Z_{CuCu}^{T}=Z_{ZrZr}^{T}=13.3$ as a result of $R_{CuZr}=1.24$(or $R_{ZrCu}=0.81$). However, the general case where a type-A atom is surrounded by both type-A and type-B atoms, has not been resolved.[24] We conjecture that the maximum coordination number for a combination of A and B atoms surrounding a type-A atom [namely, $(Z_{AB}^{max}, Z_{AA}^{max})$], can be obtained as a linear interpolation between Z_{AB}^{T} and Z_{AA}^{T}. Thus, one has

$$\frac{Z_{AB}^{max}}{Z_{AB}^{T}} + \frac{Z_{AA}^{max}}{Z_{AA}^{T}} = 1 \tag{4a}$$

and

$$\frac{Z_{BA}^{max}}{Z_{BA}^{T}} + \frac{Z_{BB}^{max}}{Z_{BB}^{T}} = 1. \tag{4b}$$

Being complementary, Z_{AB}^{max} and Z_{AA}^{max} define the most efficient local packing for the type-A atom, so do Z_{BA}^{max} and Z_{BB}^{max}

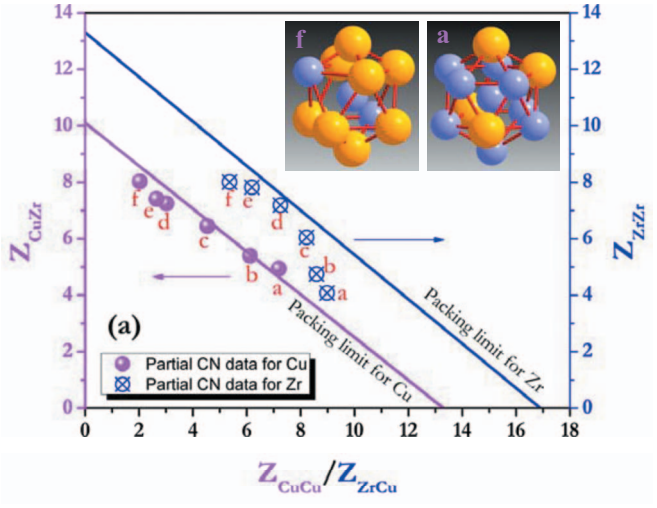

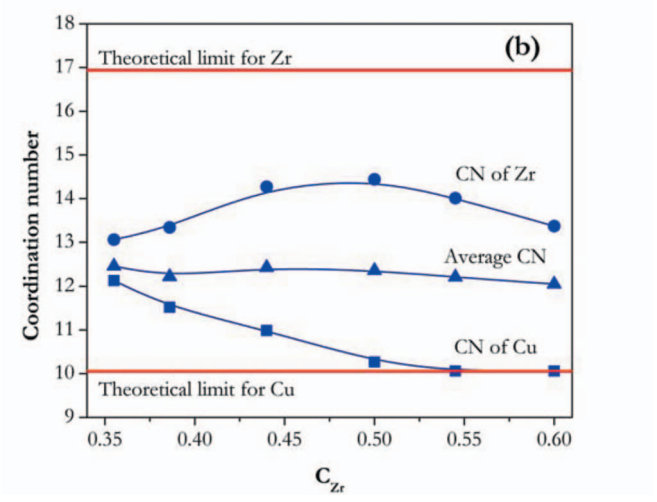

FIG. 4. (Color) (a) Plots of Z_{CuCu} vs Z_{CuZr} and Z_{ZrCu} vs Z_{ZrZr} showing the correlation between partial-coordination numbers. The two solid lines represent the efficient local packing limit for Cu and Zr, respectively, as calculated from Eq. (4a) and (4b). Letters a-f refer to $Zr_xCu_{(100-x)}$ where $x=35.5$, 38.6, 44, 50, 54.5, and 60, respectively. (b) The experimental average coordination number and the total coordination numbers of Cu and Zr as a function of composition. The two solid straight lines mark the theoretical maximum coordination number for Cu around Zr (top) and vice versa (bottom), according to the Miracle model (Ref. 5). The insets represent structures of two types of Cu-centered clusters, i.e., (0,12,0) and (2,8,0) Voronoi polyhedra as would be seen in a and f, respectively. Orange and light blue balls represent Zr and Cu atoms, respectively.

for the type-B atom. In Fig. 4(a), we plotted the linear relationship of Z_{CuCu}^{max} vs Z_{CuZr}^{max} as defined in Eq. (4a), as well as that of Z_{ZrCu}^{max} vs Z_{ZrZr}^{max} [Eq. (4b)]. Also in Fig. 4(a), we have superimposed the experimental partial CNs with respect to Cu and Zr as Z_{CuCu} vs Z_{CuZr} and Z_{ZrCu} vs Z_{ZrZr}, respectively. It can be seen that the experimental data for Cu (denoted as magenta solid circles) fall, within the experimental errors, exactly on the line of Z_{CuCu}^{max} vs Z_{CuZr}^{max} over the full composition range investigated, indicating that the local environment of Cu approaches the efficient local packing limit. This is

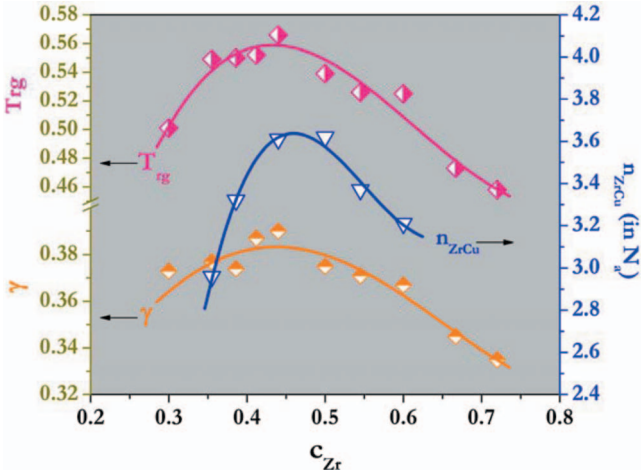

FIG. 5. (Color) Comparison of the extracted number of Zr-Cu bonds with the glass-forming ability indicators $\gamma[=T_x/(T_g+T_l)]$ and $T_{rg}(=T_g/T_l)$ as a function of alloy composition.

consistent with the observed negative values of the Warren-Cowley coefficient with respect to Cu(α_{Cu}), both suggesting the presence of Cu-centered atomic clusters. In contrast, the experimental data for Zr (denoted as blue open circles) are comparatively far away from the Z^{max}_{ZrCu} vs Z^{max}_{ZrZr} line (blue), suggesting that Zr is much less efficiently packed than Cu. Clearly, the efficiently packed Cu-centered clusters of atoms (including both Zr and Cu atoms in the first coordination shell) are the building units for all the compositions investigated. However, the respective amounts of Zr and Cu atoms in the clusters may vary to facilitate the composition change, as does the topology of the clusters. For the Cu-rich compositions, such as $Zr_{35.5}Cu_{64.5}$, the total CN of Cu$(=Z_{CuZr}+Z_{CuCu})$ reaches 12, as illustrated in Fig. 4(b). This means that this type of the Cu-centered clusters belongs to a class of 12-vertex-coordinated polyhedron, most probably being distorted icosahedron [i.e., (0,12,0)-Voronoi polyhedron] with eight Cu atoms and four Zr atoms at vertices, as shown in the inset of Fig. 4(a).[28] While for the Zr-rich compositions (above 50 at.% Zr), the total CN of Cu becomes constantly 10, reaching the maximum number (or theoretical limit) of Zr that could possibly surround Cu [see Fig. 4(b)]. The topology of this type of Cu-centered clusters would be likely a 10-vertex polyhedron, as it reaches a minimum energy for (2,8,0)-Voronoi polyhedron [i.e., bi-capped square Archimedean antiprism, see the inset of Fig. 4(a)].[28]

Compared with random packing, the efficient local atomic packing scheme in metallic glasses implies strong chemical interactions between unlike atoms and thus the increase in the number of atomic bonds. If this scheme is also valid in the liquid that forms the glass, as discussed in the introduction part (also see below), it would reduce atomic mobility and enhance the liquid's glass-forming ability. Here using the experimental CNs obtained from the diffraction study and the thermal-property data from the DSC measurements, we are able to demonstrate a correlation between unlike atom bonds and the glass-forming ability. Figure 5 shows the number of unlike atom bonds ($\bar{n}_{ZrCu}$) per mole of Zr and Cu atoms as a function of composition, in comparison with the indicators for glass-forming ability known as γ (Ref. 29) and T_{rg}.[30] Here, the number of unlike atom bonds is calculated as $\bar{n}_{ZrCu}=N_a c_{Zr} Z_{ZrCu}$, where N_a is Avogadro's number, $\gamma=T_x/(T_g+T_l)$ ranging from 0.2 to 0.5 for various glass-forming systems[29] and $T_{rg}=T_g/T_l$ ranging from 0.4 to 0.67.[30] Table I summarizes the values of T_x, T_g, T_l, γ, and T_{rg} for ten Zr-Cu glasses. It is noted from Fig. 5 and Table I that γ and T_{rg} and $\bar{n}_{ZrCu}$ follow a similar trend as a function of composition and all peak in the vicinity of 44.0 at. % Zr. This provides an experimental demonstration of the correlation between glass-forming ability and local atomic structure. The γ and T_{rg} parameters are both good gauges for the structural stability of a supercooled liquid and its resistance to crystallization.[29,30] The more stable the liquid, the greater the tendency for the liquid to form a glass. The liquid stability is primarily determined by the enthalpy of mixing (ΔH_{mix}), especially for supercooled liquids at low temperatures.[31,32] Assuming pair-wise bond energies, ΔH_{mix} scales with the number of unlike atom bonds as $\Delta H_{mix}=\bar{n}_{ZrCu}\cdot\varepsilon$,[33] where ε is a negative constant representing the difference in the bond energy between the Zr-Cu bond and the average of the Zr-Zr and Cu-Cu bonds. In fact, the observed maximum of $\bar{n}_{ZrCu}$ at ~44 at. % Zr is consistent with the thermodynamic evaluation by Abe *et al.*[34] who showed a minimum of ΔH_{mix} at ~44.0 at. % Zr at 1,000 K. Consequently, one can conclude that good glass formers favor more unlike atom bonds which increase the enthalpy of mixing and thus stabilize the liquid. This also implies that, as discussed above, the efficient local atomic packing scheme that facilitates more unlike atom bonds in the liquid and the glass is the origin of good glass-forming ability.

As shown in Fig. 3, the partial coordination numbers of the Zr-Cu glasses vary as a continuous quasilinear function of the composition in a rather wide range without any peculiarity. This contrasts with the lack of definite composition dependence of CNs for crystalline counterparts (i.e., intermetallic compounds and their mixtures), but is similar to what was observed for liquids, for instance, molten Si-transition-metal alloy.[35,36] Accordingly, the quasilinear correlation, indicative of a substitutional solution nature of Cu and Zr, is likely a manifestation of the "liquidlike" structure of metallic glasses. It has been proposed that a metallic glass is simply a frozen liquid, whose structure is an inheritance of the liquid that precedes the glass transition.[3] As one can see from the Zr-Cu phase diagram,[37] Zr and Cu are essentially insoluble in the crystalline solid state, and it is only in the liquid state that there exists one degree of freedom (i.e., composition) which allows extensive amount of mutual solubility, particularly in the glass-forming range of 35–70 at. % Zr. When such liquids *freeze* into glasses, they would *retain* the liquid structure, especially the local structure units, as well as the apparent substitutional solution nature. Thus, in addition to the structure, metallic glasses also *inherit* one degree of freedom from parent liquids, which explains why metallic glass formers are always found in a composition range, rather than a stoichiometric composition as is the case for an intermetallic compound. The implication of the liquidlike nature of metallic glasses, further supports our preceding analysis which shows that the efficient local atomic packing in a glass (i.e., maximizing the number of unlike atom bonds) indeed

have a strong correlation with the stability of the glass-forming *liquid* (i.e., the γ parameter).

V. CONCLUSIONS

We have investigated local atomic structure of Zr-Cu glasses over a wide composition range by synchrotron x ray and neutron diffraction, along with a neutron isotope substitution method. Our analysis of experimental coordination numbers revealed a scheme of efficient packing of multiple type of atoms in the first coordination shell of solute-centered clusters, which has important implications for structure modeling and simulations. We also demonstrated a clear correlation between the number of unlike atom bonds and the glass-forming ability, providing insights into the role of local atomic packing in the stability of liquids and glasses.

ACKNOWLEDGMENTS

This research was supported by the Laboratory Directed Research and Development program of Oak Ridge National Laboratory (ORNL), managed by UT-Battelle, LLC for the U.S. Department of Energy under Contract No. DE-AC05-00OR22725. Z.P.L. acknowledges the financial support from National Natural Science Foundation of China under Grant No. 50725104 and the 973 program under Contract No. 2007CB613903. Work at the Ames Laboratory was supported by the Department of Energy, Office of Basic Energy Sciences, under Contract No. DE-AC02-07CH11358. The high-energy x ray work at the MUCAT sector of the APS was supported by the U.S. Department of Energy, Office of Science, Basic Energy Sciences under Contract No. DE-AC02-06CH11357.

*Corresponding author. dongma@ornl.gov

[1] Q. Mei, C. J. Benmore, and J. K. R. Weber, Phys. Rev. Lett. **98**, 057802 (2007).
[2] C. A. Angell, K. L. Ngai, G. B. McKenna, P. F. McMillan, and S. W. Martin, J. Appl. Phys. **88**, 3113 (2000).
[3] J. C. Dyre, Nature Mater. **3**, 749 (2004).
[4] D. B. Miracle, Nature Mater. **3**, 697 (2004).
[5] D. B. Miracle, W. S. Sanders, and O. N. Senkov, Philos. Mag. **83**, 2409 (2003).
[6] H. W. Sheng, W. K. Luo, F. M. Alamgir, J. M. Bai, and E. Ma, Nature (London) **439**, 419 (2006).
[7] D. Wang, Y. Li, B. B. Sun, M. L. Sui, K. Lu, and E. Ma, Appl. Phys. Lett. **84**, 4029 (2004).
[8] D. H. Xu, B. Lohwongwatana, G. Duan, W. L. Johnson, and C. Garland, Acta Mater. **52**, 2621 (2004).
[9] M. B. Tang, D. Q. Zhao, M. X. Pan, and W. H. Wang, Chin. Phys. Lett. **21**, 901 (2004).
[10] Y. Li, Q. Guo, J. A. Kalb, and C. V. Thompson, Science **322**, 1816 (2008).
[11] D. Ma, A. D. Stoica, and X.-L. Wang, Nature Mater. **8**, 30 (2009).
[12] M. I. Mendelev, M. J. Kramer, R. T. Ott, and D. J. Sordelet, Philos. Mag. **89**, 109 (2009).
[13] A. Inoue and W. Zhang, Mater. Trans. **45**, 584 (2004).
[14] P. Lamparter, S. Steeb, and E. Grallath, Z. Naturforsch. A **38**, 1210 (1983).
[15] T. Kudo, K. Suzuki, M. Misawa, T. Mizoguchi, N. Watanabe, and N. Niimura, J. Phys. Soc. Jpn. **45**, 1773 (1978).
[16] T. Fujiwara, H. S. Chen, and Y. Waseda, J. Phys. F: Met. Phys. **13**, 97 (1983).
[17] H. S. Chen and Y. Waseda, Phys. Status Solidi A **51**, 593 (1979).
[18] R. Harris and L. J. Lewis, Phys. Rev. B **25**, 4997 (1982).
[19] A. Sadoc, D. Raoux, P. Lagarde, and A. Fontaine, J. Non-Cryst. Solids **50**, 331 (1982).
[20] N. Mattern, A. Schops, U. Kuhn, J. Acker, O. Khvostikova, and J. Eckert, J. Non-Cryst. Solids **354**, 1054 (2008).
[21] A. M. Flank, P. Lagarde, D. Raoux, J. Rivory, and A. Sadoc, Proceeding of fourth International Conference on Rapidly Quenched Metals, 1981 (unpublished) Vol. 393.
[22] J. M. Cowley, J. Appl. Phys. **21**, 24 (1950).
[23] P. F. Peterson, M. Gutmann, T. Proffen, and S. J. L. Billinge, J. Appl. Crystallogr. **33**, 1192 (2000).
[24] X. Y. Qiu, E. S. Bozin, P. Juhas, T. Proffen, and S. J. L. Billinge, J. Appl. Crystallogr. **37**, 110 (2004).
[25] T. Egami and S. J. L. Billinge, *Underneath the Bragg Peaks: Structural Analysis of Complex Materials* (Pergamon, New York, 2003).
[26] D. Ma, A. D. Stoica, L. Yang, X. L. Wang, Z. P. Lu, J. Neuefeind, M. J. Kramer, J. W. Richardson, and T. Proffen, Appl. Phys. Lett. **90**, 211908 (2007).
[27] T. Egami and Y. Waseda, J. Non-Cryst. Solids **64**, 113 (1984).
[28] V. A. Borodin, Philos. Mag. A **79**, 1887 (1999).
[29] Z. P. Lu and C. T. Liu, Phys. Rev. Lett. **91**, 115505 (2003).
[30] D. Turnbull, Contemp. Phys. **10**, 473 (1969).
[31] F. R. de Boer, R. Boom, W. C. M. Mattens, A. R. Miedema, and A. K. Niessen, *Cohesion in Metals: Transition Metal Alloys* (North-Holland, Amsterdam, 1988).
[32] Z. P. Lu, J. Shen, D. W. Xing, J. F. Sun, and C. T. Liu, Appl. Phys. Lett. **89**, 071910 (2006).
[33] D. R. Gaskell, *Introduction to Metallurgical Thermodynamics* (McGraw-Hill, New York, 1973).
[34] T. Abe, M. Shimono, M. Ode, and H. Onodera, Acta Mater. **54**, 909 (2006).
[35] Y. Kita, J. B. Vanzytveld, Z. Morita, and T. Iida, J. Phys.: Condens. Matter **6**, 811 (1994).
[36] Y. Kita, M. Zeze, and Z. Morita, Trans. Iron Steel Inst. Jpn. **22**, 571 (1982).
[37] A. I. Zaitsev, N. E. Zaitseva, J. P. Alexeeva, S. F. Dunaev, and Y. S. Nechaev, Phys. Chem. Chem. Phys. **5**, 4185 (2003).